Cancer Science

WILEY | JCA JAPANESE CANCER ASSOCIATION

ORIGINAL ARTICLE OPEN ACCESS

Carbonic Anhydrase 12 as a Novel Prognostic Biomarker and Therapeutic Target for High-Risk Follicular Thyroid Carcinoma

Masashi Tanida[1,2] | Tsuyoshi Takashima[1] | Shinichiro Tahara[1] | Masaharu Kohara[1] | Haruka Kanai[2] | Masami Suzuki[2] | Motoyuki Suzuki[2] | Mitsuyoshi Hirokawa[3] | Ayana Suzuki[3] | Shinya Sato[4] | Daisuke Okuzaki[5] | Satoshi Nojima[1] | Takahiro Matsui[1] | Hidenori Inohara[2] | Eiichi Morii[1]

[1]Department of Pathology, Graduate School of Medicine, The University of Osaka, Osaka, Japan | [2]Department of Otorhinolaryngology-Head and Neck Surgery, Graduate School of Medicine, The University of Osaka, Osaka, Japan | [3]Department of Diagnostic Pathology and Cytology, Kuma Hospital, Kobe, Japan | [4]Department of Surgery, Yamashita Thyroid Hospital, Fukuoka, Japan | [5]Single Cell Genomics, Human Immunology, WPI Immunology Frontier Research Center, The University of Osaka, Osaka, Japan

Correspondence: Eiichi Morii (morii.eiichi.med@osaka-u.ac.jp)

Received: 5 September 2025 | **Revised:** 22 October 2025 | **Accepted:** 29 October 2025

Funding: This work was supported by AMED under Grant Number JP21ae0121049 and by JSPS KAKENHI Grant Numbers T23K273910.

Keywords: biomarkers | carbonic anhydrase 12 | follicular thyroid carcinoma | lenvatinib | matrix metalloproteinase 2

ABSTRACT

Follicular thyroid carcinoma is generally associated with a favorable prognosis; however, a subset of follicular thyroid carcinoma shows poor prognosis and frequent distant metastases, and this subset is referred to as high-risk follicular thyroid carcinoma. Difficulty in distinguishing high-risk from low-risk follicular thyroid carcinoma based on current diagnostic approaches leads to the overtreatment of patients with indolent disease. Therefore, the identification of novel biomarkers capable of reliably distinguishing high-risk follicular thyroid carcinoma is essential for accurate risk stratification. Such biomarkers may serve as therapeutic targets for metastatic follicular thyroid carcinoma. This study aimed to identify novel prognostic markers and therapeutic targets for high-risk follicular thyroid carcinoma. In this study, we conducted bulk ribonucleic acid sequencing of high-risk follicular thyroid carcinoma, including widely invasive subtypes and metastatic tumors, and we identified carbonic anhydrase 12 as a candidate biomarker. Immunohistochemical analysis revealed significantly higher carbonic anhydrase 12 expression in follicular thyroid carcinoma than in benign follicular adenomas, particularly in widely invasive and encapsulated angioinvasive subtypes. High carbonic anhydrase 12 expression was an independent predictor of poor disease-free survival, surpassing conventional clinicopathological parameters. Functional assays showed that carbonic anhydrase 12 promoted follicular thyroid carcinoma proliferation, invasion, and migration partly by regulating matrix metalloproteinase 2 expression. Furthermore, carbonic anhydrase 12 inhibitor U104 suppressed follicular thyroid carcinoma cell growth in a dose-dependent manner, and its combination with lenvatinib exerted synergistic antiproliferative effects. Collectively, these findings identified carbonic anhydrase 12 as a novel prognostic biomarker of follicular thyroid carcinoma and a promising therapeutic target.

Abbreviations: CA12, carbonic anhydrase 12; CCLE, cancer cell line encyclopedia; CO_2, carbon dioxide; DEGs, differentially expressed genes; DFS, disease-free survival; EA, encapsulated angioinvasive (subtype of FTC); ECM, extracellular matrix; FA, follicular adenoma; FTC, follicular thyroid carcinoma; HALO, head alignment optimization (image analysis software); HE, hematoxylin and eosin; IHC, immunohistochemistry; KD, knockdown; MI, minimally invasive (subtype of FTC); MMP, matrix metalloproteinase; OS, overall survival; PTC, papillary thyroid carcinoma; RNA, messenger ribonucleic acid; RNA-seq, RNA sequencing; RT-qPCR, reverse transcription quantitative polymerase chain reaction; shRNA, short hairpin RNA; WHO, world health organization; WI, widely invasive (subtype of FTC).

1 | Introduction

Thyroid carcinoma is the most common endocrine malignancy, with its incidence steadily increasing, becoming the ninth most commonly diagnosed carcinoma worldwide [1]. Follicular thyroid carcinoma (FTC) is the second most common histological subtype of thyroid carcinoma, with a prevalence of 5%–10% after papillary thyroid carcinoma (PTC) [1, 2]. FTC can be distinguished from benign follicular adenoma (FA) based on the presence of capsular invasion, vascular invasion, or distant metastasis. The WHO Classification categorizes FTC into three subtypes based on the invasive pattern: minimally invasive (MI), encapsulated angioinvasive (EA), and widely invasive (WI) subtypes [2, 3]. Although PTC primarily metastasizes to the regional lymph nodes, FTC exhibits a higher propensity for distant metastasis. FTC is generally associated with a favorable prognosis; however, several cases demonstrate frequent metastases and poorer outcomes [4]. Clinicopathological risk factors, such as age [5, 6], sex [7, 8], tumor size [9], postoperative histopathological type [9, 10], and Ki67 staining [11], are reportedly linked to poor prognosis. In particular, the postoperative histopathological subtype is emphasized in the current treatment guidelines. However, accurately identifying patients at risk of poor prognosis remains difficult, leading to excessive operations and overtreatment of low-risk patients with indolent disease [12]. Therefore, novel prognostic biomarkers are urgently needed to accurately stratify patients, guide more aggressive therapy for high-risk cases, and prevent overtreatment of low-risk cases. Furthermore, identifying therapeutic targets that prevent metastasis and inhibit tumor cell growth is crucial. Such biomarkers of high-risk FTC may also serve as potential therapeutic targets. This study aimed to identify novel prognostic markers and therapeutic targets for high-risk FTC.

We enrolled FTCs with metastatic or WI subtypes as high-risk and performed bulk RNA sequencing (RNA-seq) on such cases. We identified carbonic anhydrase 12 (CA12), a member of a superfamily of metalloenzymes that catalyzes the conversion of CO_2 to bicarbonate and protons [13], as a prognostic biomarker and potential therapeutic target for high-risk FTC.

2 | Material and Methods

2.1 | Patients

Bulk RNA-seq was done on 8 cases of high-risk FTC showing distant metastases or WI subtypes surgically resected at The University of Osaka Hospital or Yamashita Thyroid Hospital. The details of these 8 cases are summarized in Table S1. In addition, we immunohistochemically studied 75 cases of thyroid follicular tumors surgically resected at Kuma Thyroid Hospital between 2008 and 2012, which included 25 cases of FA and 50 cases of FTC (25 MI, 7 EA and 18 WI subtypes). The details of these 8 cases are summarized in Table S2. This research was approved by the Ethics Review Board of the Graduate School of Medicine, The University of Osaka (No. 849).

2.2 | RNA Sequencing Analysis of FFPE Samples

Formalin-fixed paraffin-embedded (FFPE) sections (10 μm) were cut, and tumor cells and the adjacent normal tissues were subjected to RNA-seq analysis. Total RNA was extracted using the miRNeasy FFPE Kit (Qiagen, Hilden, Germany) in accordance with the manufacturer's protocol. NGS library preparation was performed using the SMARTer Stranded Total RNA Sample Prep Kit-Pico Input Mammalian (Clontech, TaKaRa) according to the manufacturer's instructions. Sequencing was performed on an Illumina NovaSeq 6000 platform in 151-base paired-end mode. Before mapping to the genome, the adapter sequences were removed with the trimmomatic software version 0.39. Sequenced reads were mapped to the human reference genome sequence (GRCh38_p13) using hisat version 2.1.0, in combination with Bowtie 2 version 2.2.3. Fragments per kilobase of exon per million mapped fragments (FPKM) were calculated using Cufflinks version 2.2.1. Raw data have been deposited in the NCBI Gene Expression Omnibus database (GSE305211). The numerical data used for analysis are filed in Tables S3 and S4.

2.3 | Public Data Analysis of Bulk RNA-Seq

Bulk RNA-Seq datasets were downloaded from the GEO datasets GSE126698 [14] and PRJEB11591 [15]; CA12 expression levels were compared between FTC, FA, and adjacent normal tissue.

2.4 | Cell Culture and Chemicals

Thyroid carcinoma cell lines FTC133, FTC238, and RO82-W-1 were purchased from The European Collection of Authenticated Cell Cultures (ECACC), T32, T41, and T85 from American Type Culture Collection (ATCC), and H8505C and IHH4 from Health Science Research Resources Bank (Osaka, Japan). All cell lines were cultured in DMEM/Ham's F-12 (08460-95, Nacalai Tesque) containing 10% fetal bovine serum (FBS) (35-010-CV, Corning) and 100 IU/mL penicillin (22-18132, FUJIFILM Wako Pure Chemical), and 100 μg/mL streptomycin (194-08512, Nacalai Tesque). They were maintained at 37°C in 5% CO_2. Chemicals used in this study were as follows: U104 (HY-13513, MedChemExpress), Lenvatinib (S1164, SelleckChem), which were dissolved in DMSO with the final concentration of DMSO in culture medium not exceeding 0.1%.

2.5 | CA12-Knockdown FTC Cells Generation Using Short Hairpin RNA (shRNA)

We constructed CA12-knockdown cells using two types of shRNA: MISSION shRNA #1 (catalog TRCN0000116249, target sequence: CCGGGTGATAACAAGGGAGTCATTTCTCGAGAAATGACTCCCTTGTTATCACTTTTTG, referred to as "CA12-KD#1") and MISSION shRNA #2 (catalog TRCN0000116250, target sequence: CCGGCCATTATAACTCAGACCTTTACTCGAGTAAAGGTCTGAGTTATAATGGTTTTTG, referred to as "CA12-KD#2") (Merck). Lentivirus encoding shRNA targeting

CA12 was produced using Lenti-X 293T cells (632180, Takara, Shiga, Japan). We mixed Lentiviral High Titer Packaging Mix (6194, Takara), Opti-MEM (31985062, Thermo Fisher Scientific), and TransIT-293 Transfection Reagent (MIR2705, Takara). The Lenti-X 293 T cells were then transfected, and the supernatant medium was collected after 48 h and filtered through a 0.22-μm filter. After introducing lentivirus using supernatant, puromycin selection was performed for 5 days to isolate transfected clones, and stable CA12-knockdown thyroid follicular cells (FTC133, FTC238) were constructed.

2.6 | Generation of CA12 Knockdown-Rescue FTC Cells Using Lentiviral Vector Plasmid

Lentiviral production of the following vectors was carried out according to the lentiviral production method above, using lentiviral vector plasmids, pLV[Exp]-EGFP-EF1A > hCA12[NM_001218.5] (VB-1312ftg, Vector Builder), pLV-EGFP-EF1A > ORF stuffer (referred to as "NV") (VB900124-3812qdj, Vector Builder) purchased from Vector Builder (Chicago, IL, USA).

2.7 | Antibodies

The primary antibody used was anti-CA12 (CL0278, AMAb90637, Atlas Antibodies). Anti-ACTB antibody (1:1000, 5125, Cell Signaling Technology) was used as a loading control. For immunohistochemistry (IHC), the anti-CA12 antibody was used at a dilution of 1:1600. The secondary antibody for IHC was EnVision+/HRP, Mouse, Immunohistochemistry Visualization (K4001, DAKO). For Western blotting, the anti-CA12 and anti-ACTB antibodies were used at a dilution of 1:1000. Horseradish peroxidase (HRP)-conjugated secondary antibodies used were Anti-Rabbit IgG (H + L), pAb-HRP (1:1000, 458, MBL), and Anti-Mouse IgG (H + L), pAb-HRP (1:1000, 330, MBL).

2.8 | RNA Extraction and RT-qPCR Analysis

Total RNA was extracted from cultured FTC cells using RNAiso Plus (9109, Takara). A quantity of 1000 ng of total RNA was converted to complementary DNA (cDNA) using the SuperScript III First-Strand Synthesis System (18080051, Thermo Fisher Scientific), following the manufacturer's instructions. Reverse Transcription quantitative Polymerase Chain Reaction (RT-qPCR) assays were performed using TaqMan Fast Advanced Master Mix (4444965, Thermo Fisher Scientific) on the StepOnePlus System (Thermo Fisher Scientific). TaqMan probes of each target were as follows: CA12 (Hs01080909_m1, 4331182, Thermo Fisher Scientific), MMP2 (Hs01548727_m1, 4331182, Thermo Fisher Scientific), ACTB (Hs99999903_m1, 4331182, Thermo Fisher Scientific). The ACTB housekeeping gene was used for normalization.

2.9 | IHC Staining

FFPE tissues were cut at a thickness of 4 μm, deparaffinized in xylene, and then rehydrated through graded ethanol solutions. They were subsequently rinsed in water. IHC staining was performed using the Dako Autostainer Link 48 (Agilent Technologies), following the manufacturer's instructions. The slides were incubated with the primary antibody for 30 min, followed by the secondary antibody for 20 min. Signals were detected by staining with DAB (DM803 + DM827/K8023, DAKO) for 10 min, followed by counterstaining with hematoxylin.

2.10 | Scoring of IHC Staining

Stained slides were scanned and photographed at 20× magnification using a NanoZoomer 2.0-HT (Hamamatsu Photonics). Whole-slide images were analyzed using HALO v3.5 software (Indica Labs). The expression scores for CA12 were calculated using the *H* score of the software. The *H* score was calculated using the following formula: (% tumor cells of strong positive) × 3 + (% tumor cells of moderate positive) × 2 + (% tumor cells of weak positive) × 1.

2.11 | Western Blotting

Dish-seeded cells were collected using 0.25% Trypsin (32777-44, Nacalai Tesque) and washed twice with phosphate-buffered saline (PBS). The cells were lysed in lysis buffer [1% NP-40 (25223-04, Nacalai Tesque), 20 mM Tris–HCl, 150 mM NaCl, and 1 mM EDTA] containing PhosSTOP (4906837001, Roche) and cOmplete Protease Inhibitor Cocktail (04693159001, Roche) and were sonicated for 10 s. The cells were then centrifuged at 13,000 rpm for 10 min. After collecting the supernatant, an equal volume of 2× sodium dodecyl sulfate (SDS) buffer (7% SDS, 140 mM Tris–HCl, 20% glycerol, 0.01% bromophenol blue, and 10% 2-mercaptoethanol) was added. Protein samples were then heated at 98°C for 5 min. Electrophoresis was performed on 5%–20% gradient SDS-polyacrylamide gels (ATTO, Tokyo, Japan). Proteins were transferred to polyvinylidene fluoride membranes using a semi-dry fashion. Membranes were then incubated with primary antibodies (as detailed in Section 2.7) for 1 h, followed by the indicated appropriate HRP-conjugated secondary antibodies (as detailed in Section 2.7) for 30 min. The HRP signals were visualized with Chemi-Lumi One Super reagents (02230–30, Nacalai Tesque). Images were acquired using an imaging system (ChemiDoc Touch, Bio-Rad, Hercules, CA, USA).

2.12 | Proliferation Assay

FTC cells were seeded at 3000 cells per well in a 96-well plate (Greiner Bio-One). Cell numbers were monitored at 0, 2, and 4 days using the Cell Counting Kit-8 (TN654, Dojindo Laboratories), following the manufacturer's instructions. The absorbance at 450 nm was measured using an SH-9000 Lab microplate reader (Hitachi, Tokyo, Japan) after 60 min of incubation.

2.13 | Matrigel Invasion Assay

Tumor cell invasion was performed using a Corning BioCoat Matrigel Invasion Chamber (Corning Inc.). Tumor cells were

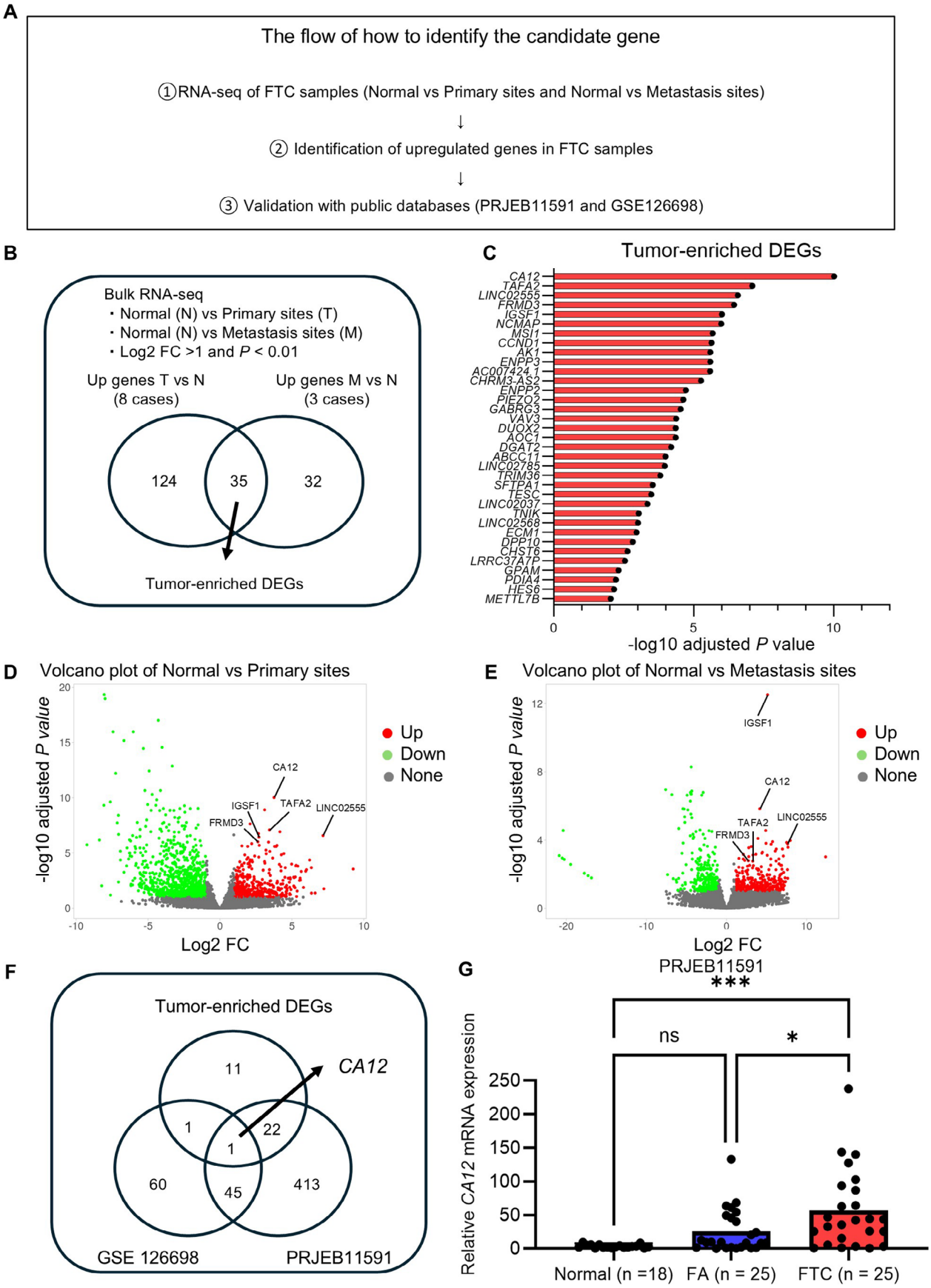

FIGURE 1 | Legend on next page.

FIGURE 1 | *CA12* mRNA is upregulated in the FTC tissues of both primary and metastatic sites. (A) Workflow for identifying candidate genes. (B) Venn diagrams of DEGs identified by RNA-seq comparing primary sites vs. normal thyroid tissues and metastasis sites vs. normal thyroid tissues. The cutoff values were log2 FC > 1, $p < 0.01$. (C) The 35 highly expressed RNAs (tumor-enriched DEGs) in both primary and metastatic sites are listed and ranked by their p value in comparison between primary tumors and normal thyroid tissues. (D, E) Volcano plots of DEGs between primary sites vs. normal thyroid tissues and metastasis sites vs. normal thyroid tissues. The top five tumor-enriched DEGs are labeled. (F) Venn diagrams of tumor-enriched DEGs and DEGs highly expressed in FTC by public bulk RNA-seq (GSE126698, PRJEB11591). The cutoff values were log2FC > 1, $p < 0.05$. (G) Relative CA12 mRNA expression in 25 FTC, 25 FA, and 18 adjacent normal thyroid tissues from the PRJEB11591 dataset. Asterisks indicate significant differences as determined using Tukey's multiple comparisons test. *$p < 0.05$, ***$p < 0.001$, ns: Not significant. DEGs, differentially expressed genes; CA12, carbonic anhydrase 12; FTC, follicular thyroid carcinoma.

seeded at 1×10^5 cells in the upper chamber of FBS-free DMEM and incubated at 37°C for 24 h. The lower chamber contained DMEM with 10% FBS. Infiltrating cells were stained with Diff-Quik (Sysmex). The number of infiltrating cells was counted in 5 random fields per chamber at high magnification.

2.14 | Wound-Healing Assay

FTC cells were seeded in 12-well plates and incubated until confluent. A scratch was applied across the well using sterile 200 μL pipette tips (Watson, Tokyo, Japan). Migration distance was calculated by subtracting the 12-h wound width from the 0-h wound width.

2.15 | Preparation of Cell Blocks for FTC133 Cells

FTC133 cells were fixed in 10% formaldehyde neutral buffer solution for 2 days and then washed with PBS, centrifuged, and pre-embedded in agarose gel (5003, Takara), before undergoing paraffin embedding with the same method used for tissue sample processing.

2.16 | Statistical Analysis

Statistical differences were evaluated using JMP Pro software version 17.0 (SAS Institute) and GraphPad Prism 10. OS and DFS rates were analyzed using a Kaplan–Meier curve and log-rank test using JMP Pro software version 17.0. Multivariate analysis was based on the Cox proportional hazards method using GraphPad Prism 10. The Volcano Plot for differential gene expression was generated using iDEP (Integrated Differential Expression Analysis Platform) version 0.96 [16]. Unless otherwise stated, results are expressed as the mean ± SD of triplicate replicates. $p < 0.05$ was considered statistically significant.

3 | Results

3.1 | *CA12* mRNA Is Highly Expressed in FTC Cases

The flowchart illustrating the search for candidate genes related to FTC aggressiveness is shown in Figure 1A. We enrolled eight cases of high-risk FTC and identified 35 differentially expressed genes (DEGs) using RNA-seq that were highly expressed in both primary and distant metastatic sites compared to the adjacent normal thyroid tissues (Figure 1B). Tumor-enriched DEGs were ranked by their p value in the comparison between primary tumors and normal thyroid tissues (Figure 1C). The top five DEGs (*CA12*, *TAFA2*, *LINC02555*, *FRMD3*, and *IGSF1*) are labeled in the volcano plots (Figure 1D,E). Among the tumor-enriched DEGs, only *CA12* showed consistently high expression in both the GSE126698 and PRJEB11591 datasets (Figure 1F). In the dataset PRJEB11591, including both carcinoma and adenoma, *CA12* expression was significantly higher in FTC than in FA (Figure 1G).

3.2 | CA12 Expression Is Higher in More Malignant Histopathological Subtypes of FTC

We immunohistochemically examined CA12 expression in 75 cases (50 FTC and 25 FA cases). CA12 expression was detected in nearly all tumor cells, including those in the invasive area, but not in the adjacent normal thyroid cells on the IHC image of the representative WI FTC case (Figure 2A). We quantified CA12 expression using Head Alignment Optimization (HALO) software (Figure 2B). The *H*-score for CA12 expression was significantly higher in FTC cases than in FA cases (Figure 2C). Among the FTC subtypes, WI and EA showed significantly higher CA12 expression than MI (Figure 2D). Among FA, several cases showed high CA12 expression, but no significant histopathological differences were detected between high and low CA12 cases. IHC staining intensity for CA12 correlated with the degree of tumor malignancy across different histopathological types (Figure 2E). Table 1 summarizes the association between CA12 expression levels and the clinicopathological features of FTC. In this study, the CA12 expression level correlated only with histopathological type, but not with other factors, such as age, sex, and tumor size.

3.3 | High CA12 Expression Is an Independent Poor Prognostic Factor in FTC

CA12 expression was evaluated in 50 FTC cases (25 MI, 7 EA, and 18 WI) using HALO (Figure 3A) and classified into high- and low-CA12 groups based on *H* scores (Figure 3B). The median *H*-score of 20 served as the cut-off value. There was no statistically significant difference in the overall survival (OS) rate ($p = 0.11$) (Figure 3C); however, the high-CA12 group exhibited a lower disease-free survival (DFS) rate than the low-CA12 group ($p = 0.026$) (Figure 3D). Univariate and multivariate Cox regression analyses demonstrated that CA12 and age were independent poor prognostic factors for DFS

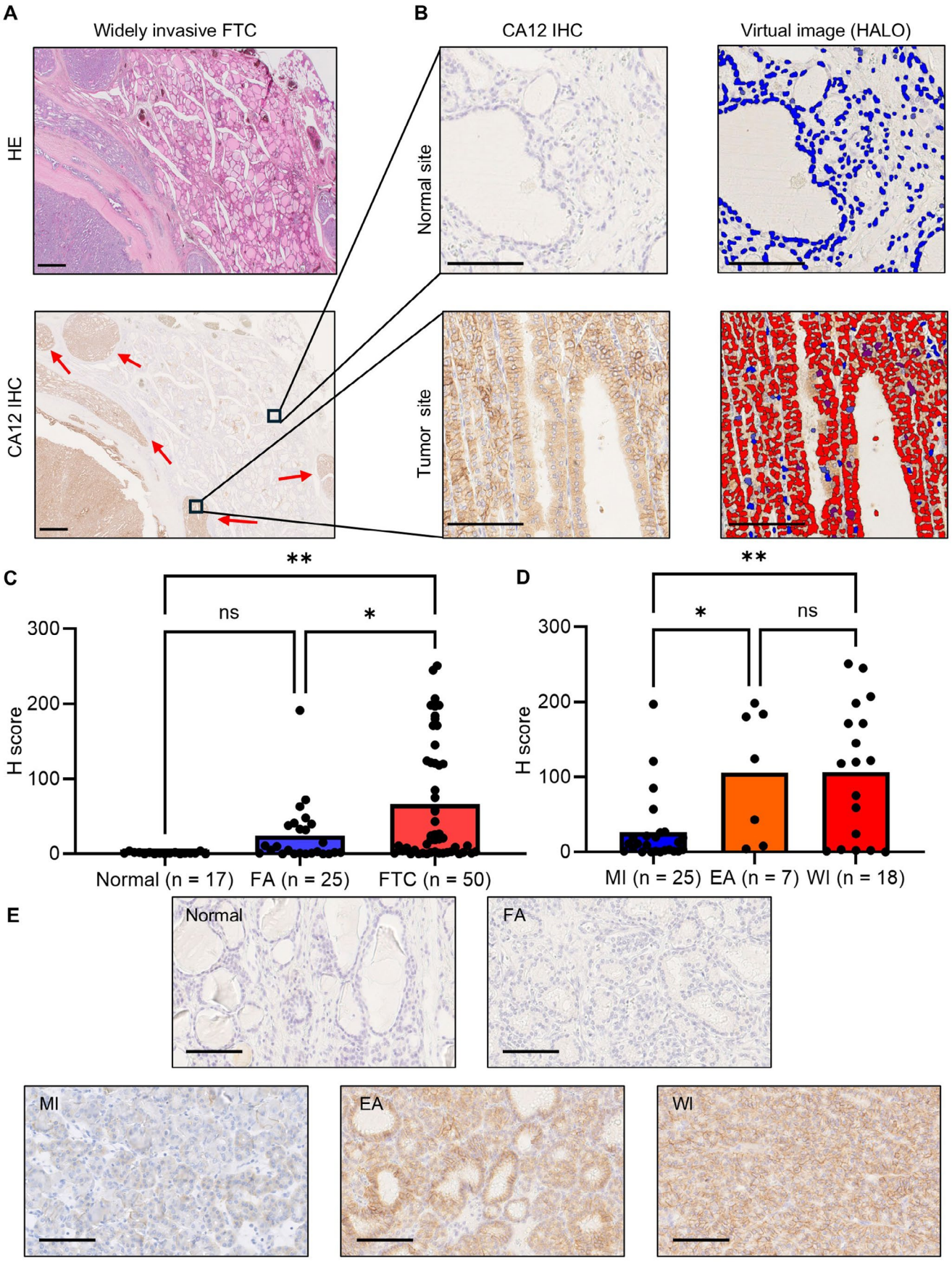

FIGURE 2 | Legend on next page.

FIGURE 2 | CA12 is more highly expressed in FTC than in FA and is strongly stained in more malignant histopathological subtypes in FTC. (A) Representative WI FTC images: HE staining (top) and CA12 IHC (bottom). Red arrows indicate the invasion areas outside the capsule. Scale bars: 1 mm. (B) Zoomed IHC images of the tumor and the normal site (left), and zoomed virtual composite images after HALO software analysis of the tumor and the normal site (right) are shown. Scale bars: 100 μm. (C, D) Bar graphs of *H* scores comparing FTC, FA, and normal thyroid tissue (C) and comparing FTC histopathological subtypes (D). Asterisks indicate significant differences as determined using Tukey's multiple comparisons test. (E) The CA12 IHC images of the median case of each histopathological subtype. Scale bars = 100 μm. *$p < 0.05$, **$p < 0.01$, ns: Not significant. CA12, carbonic anhydrase 12; EA, encapsulated angioinvasive; FTC, follicular thyroid carcinoma; IHC, immunohistochemistry; MI, minimally invasive; WI, widely invasive.

TABLE 1 | Correlation between CA12 and clinicopathological parameters.

Parameters		CA12 High	CA12 Low	*p*
Age				
< 55	27	13	14	
≥ 55	23	12	11	1
Sex				
Female	38	19	19	
Male	12	6	6	1
Pathology				
MI	25	7	18	
EA or WI	25	18	7	0.004
T stage				
pT1 or pT2	32	21	17	
pT3	12	4	8	0.32
Lymph metastasis at diagnosis				
N+	0	0	0	
N−	50	25	25	N/A
Distant metastasis at diagnosis				
M+	4	4	0	
M−	46	21	25	0.11
Ki67				
< 5%	34	16	18	
≥ 5%	16	9	7	0.76

in patients with FTC (Figure 3E). Furthermore, CA12 levels were significantly higher in patients with metastases than in those without (Figure 3F).

3.4 | CA12 Altered Matrix Metalloproteinase-2 (MMP-2) Expression and Regulated the Proliferation, Migration, and Invasion of FTC Cells

We evaluated CA12 expression in the following thyroid carcinoma cell lines: FTC133, FTC238, and RO82W1 (follicular); T32, T41, and T85 (papillary); and 8505C and IHH4 (anaplastic), using reverse transcription quantitative polymerase chain reaction (RT-qPCR) and western blotting. CA12 expression was higher in FTC cell lines, especially FTC133 and FTC238, than in anaplastic or papillary carcinoma cell lines (Figure 4A). To investigate the function of CA12, we used FTC133 and FTC238 cells to downregulate *CA12* by transfecting two *CA12*-specific shRNAs (shCA12-KD#1 and shCA12-KD#2). Transfection efficiency was examined using RT-qPCR and western blotting (Figure 4B). We also confirmed the knockdown of CA12 using FTC133 cell blocks (Figure 4C). CA12 silencing significantly reduced the proliferation of FTC cells (Figure 5A; **$p < 0.01$). Furthermore, CA12 knockdown reduced FTC cells' invasion and migration rates (Figure 5B,C; *$p < 0.05$, **$p < 0.01$). Next, we rescued CA12 expression in FTC-knockdown cells (Figure 6A) and found that invasion and proliferation were recovered by CA12 overexpression (Figure 6B,C). Because MMPs are known to be responsible for invasion, we next examined the relationship between CA12 and MMPs. Using the CCLE-Broad-MIT database on the CellMiner web application (https://discover.nci.nih.gov/cellminercdb/), we found that *MMP2* correlated with *CA12* (Pearson correlation (r) = 0.84, $p = 0.0006$; Figure 6D). The raw data are summarized in Table S5. CA12 knockdown significantly reduced *MMP2*, which was restored by the overexpression of CA12 (Figure 6E).

3.5 | CA12 Inhibitor U104 Reduced FTC Cell Proliferation and Enhanced the Effect of Lenvatinib

We investigated the pharmacological effects of the CA12 inhibitor U104 on FTC cells. Treatment with U104 reduced FTC133 growth in a dose-dependent manner (Figure 7A). Lenvatinib, a multi-targeted tyrosine kinase inhibitor used as a standard treatment for metastatic FTC [17], also inhibited FTC133 proliferation (Figure 7B). Although U104 (50 μM) or lenvatinib (5 μM) alone did not significantly affect FTC133 proliferation, their combination significantly inhibited proliferation (Figure 7C). These findings suggest that CA12 is a potential therapeutic target for high-risk FTC.

4 | Discussion

FTC is generally associated with a favorable prognosis; however, a subset shows poor outcomes and frequent distant metastases [18]. Novel prognostic markers to distinguish high-risk FTC would help prevent the overtreatment of patients, as surgical resection is typically performed for all FTC cases, including indolent ones [12]. Such biomarkers may also serve as potential

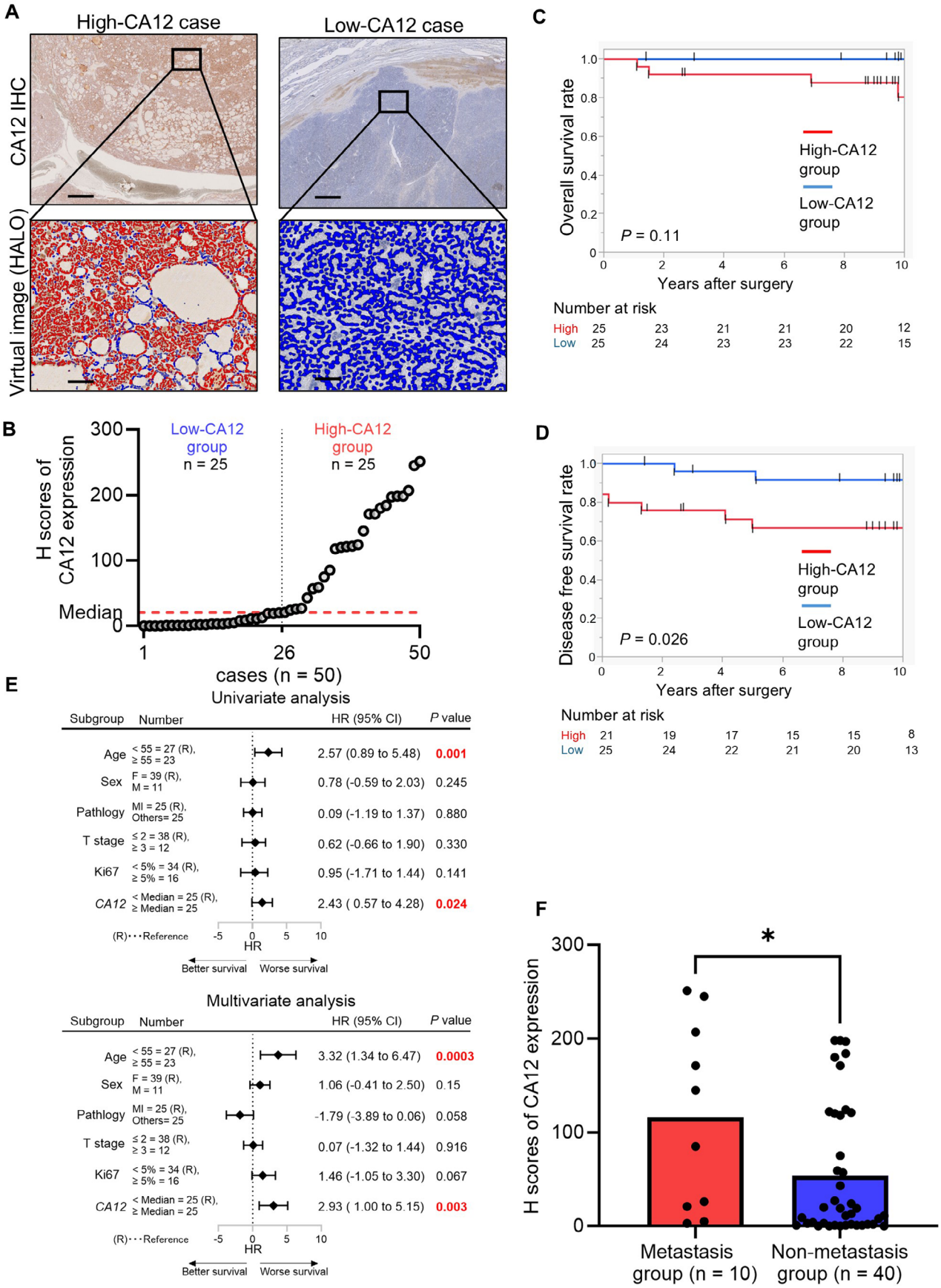

FIGURE 3 | Legend on next page.

FIGURE 3 | CA12 is an independent poor prognostic factor in FTC. (A) Representative CA12 IHC images of FTC samples in the high-CA12 and low-CA12 groups. Zoomed CA12 IHC images top and composite images analyzed with HALO software (bottom) are shown. Scale bars = 1 mm in upper panels, 100 μm in lower panels. (B) Plots of CA12 expression in FTC cases ($n = 50$). The median served as the cutoff value. (C, D) Kaplan–Meier curves for overall survival (C) and disease-free survival (D) in the high- ($n = 25$) and low-CA12 ($n = 25$) groups. p values were determined by the log-rank test ($p = 0.11$ for OS and $p = 0.026$ for DFS). (E) Forest plots of univariate and multivariate Cox regression analyses of CA12 expression and clinical features. *p-values* were determined by the Cox proportional hazards method. (F) Bar graph of CA12 expression in the metastasis group ($n = 10$) and the non-metastasis group ($n = 40$). *$p < 0.05$. Asterisks indicate significant differences as determined using Student's t-test. CA12, carbonic anhydrase 12; FTC, follicular thyroid carcinoma; IHC, immunohistochemistry.

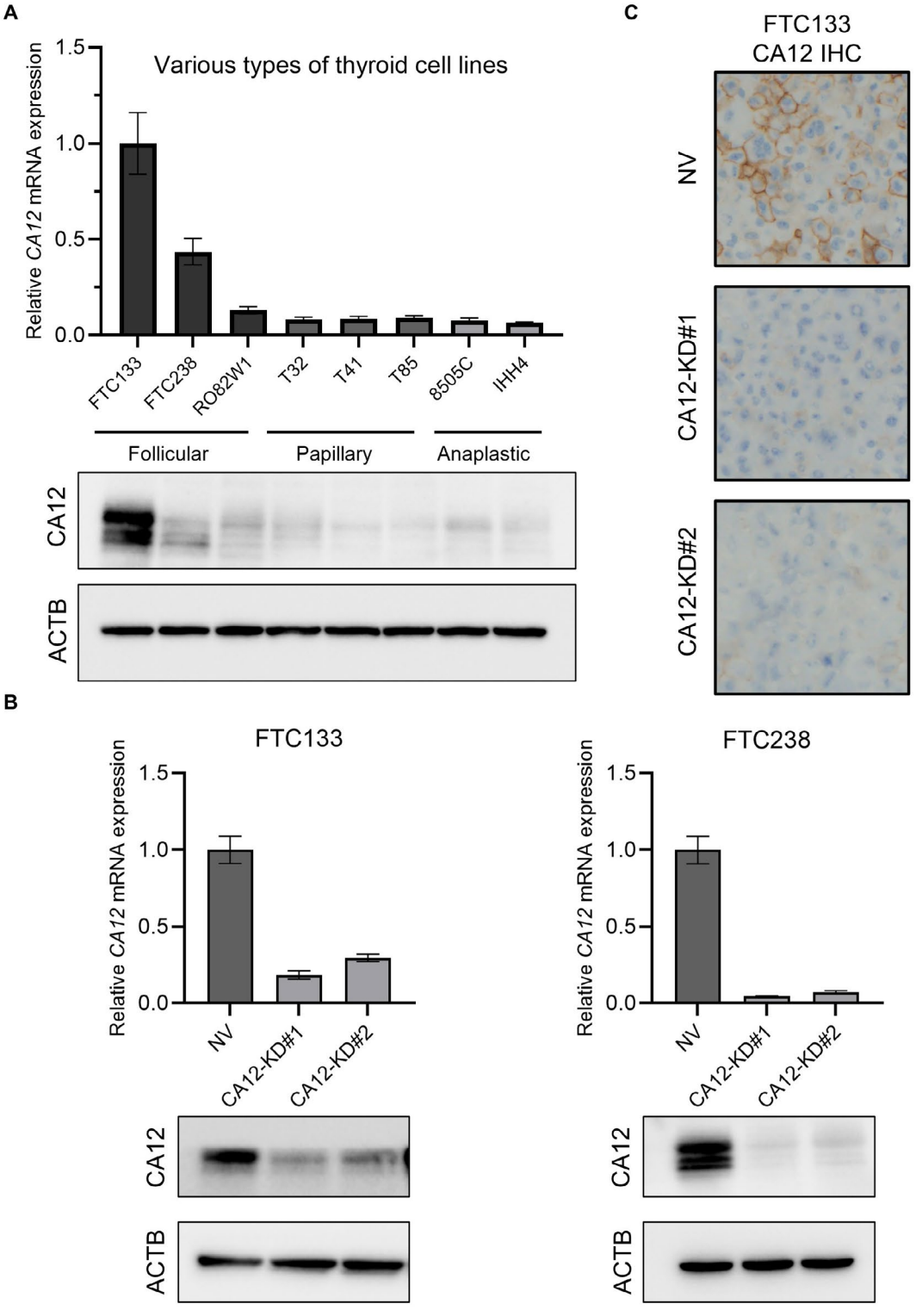

FIGURE 4 | Legend on next page.

FIGURE 4 | Generation of CA12 knockdown FTC133 and FTC238 cells. CA12 knockdown cells were generated using shRNA vectors. (A) Analysis of CA12 expression in thyroid carcinoma cell lines by RT-qPCR (top) and western blotting (bottom). CA12 was more highly expressed in thyroid follicular cancer cell lines, especially FTC133 and FTC238, than in anaplastic or papillary carcinoma cell lines. (B) Confirmation of CA12 knockdown (KD) in FTC133 and FTC238 cells (CA12-KD#1 and CA12-KD#2) by RT-qPCR and western blotting. (C) CA12 IHC images of the FTC133 cells (NV, CA12-KD#1, and CA12-KD #2). CA12, carbonic anhydrase 12; FTC, follicular thyroid carcinoma; IHC, immunohistochemistry; RT-qPCR, reverse transcription quantitative polymerase chain reaction.

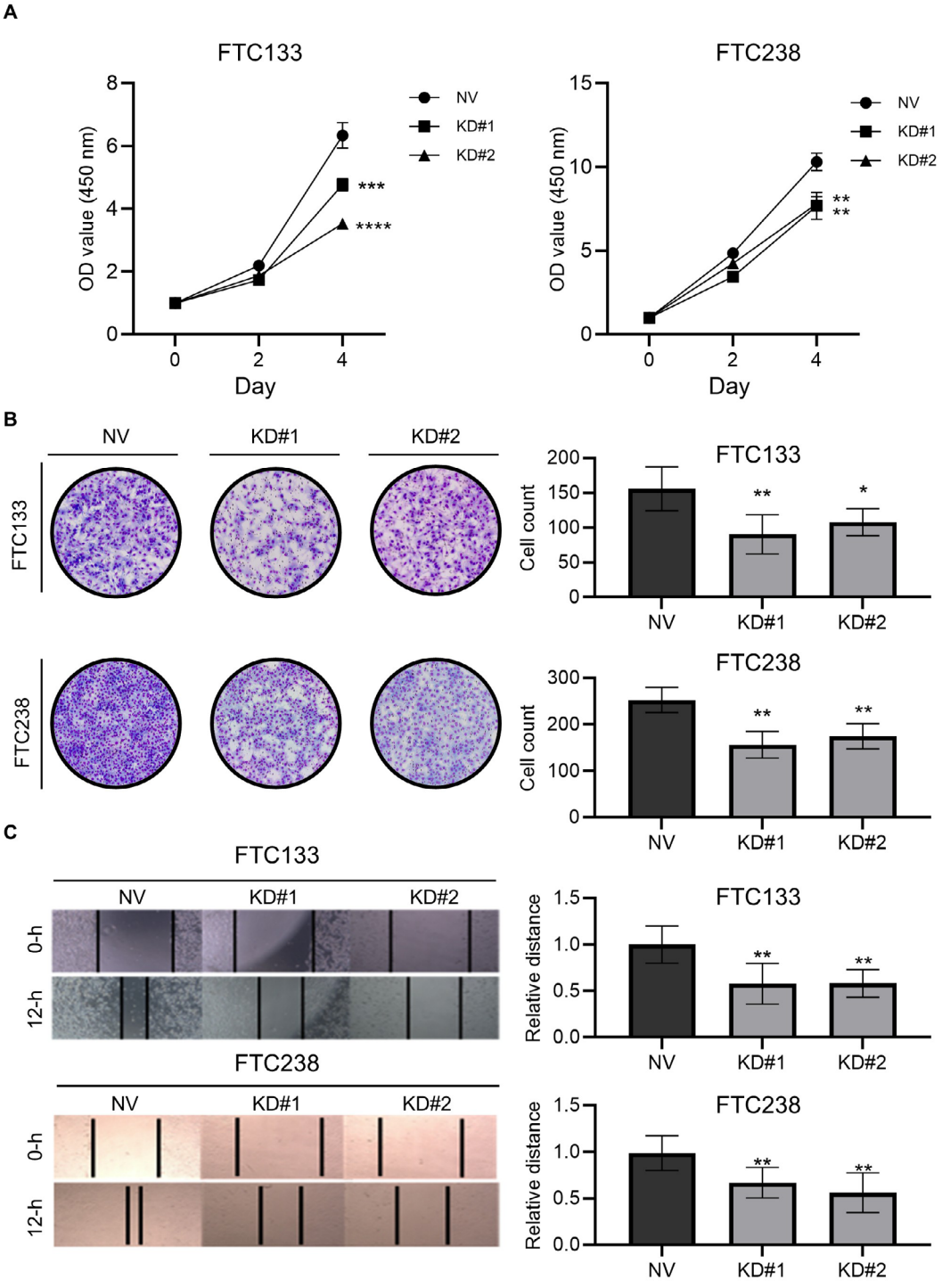

FIGURE 5 | CA12 regulates the proliferation, migration, and invasion of FTC cells. (A) Cell proliferation assay using CCK8. (B) Matrigel invasion assay. Representative images of infiltrating cells are shown. Infiltrating cells were counted in five random fields per well and plotted. (C) Wound-healing assay. Migration distance was calculated by subtracting the 12-h wound width from the 0-h wound width. Asterisks indicate significant differences (Student's *t*-test): $*p < 0.05$, $**p < 0.01$, $***p < 0.001$, $****p < 0.0001$. CA12, carbonic anhydrase 12; FTC, follicular thyroid carcinoma.

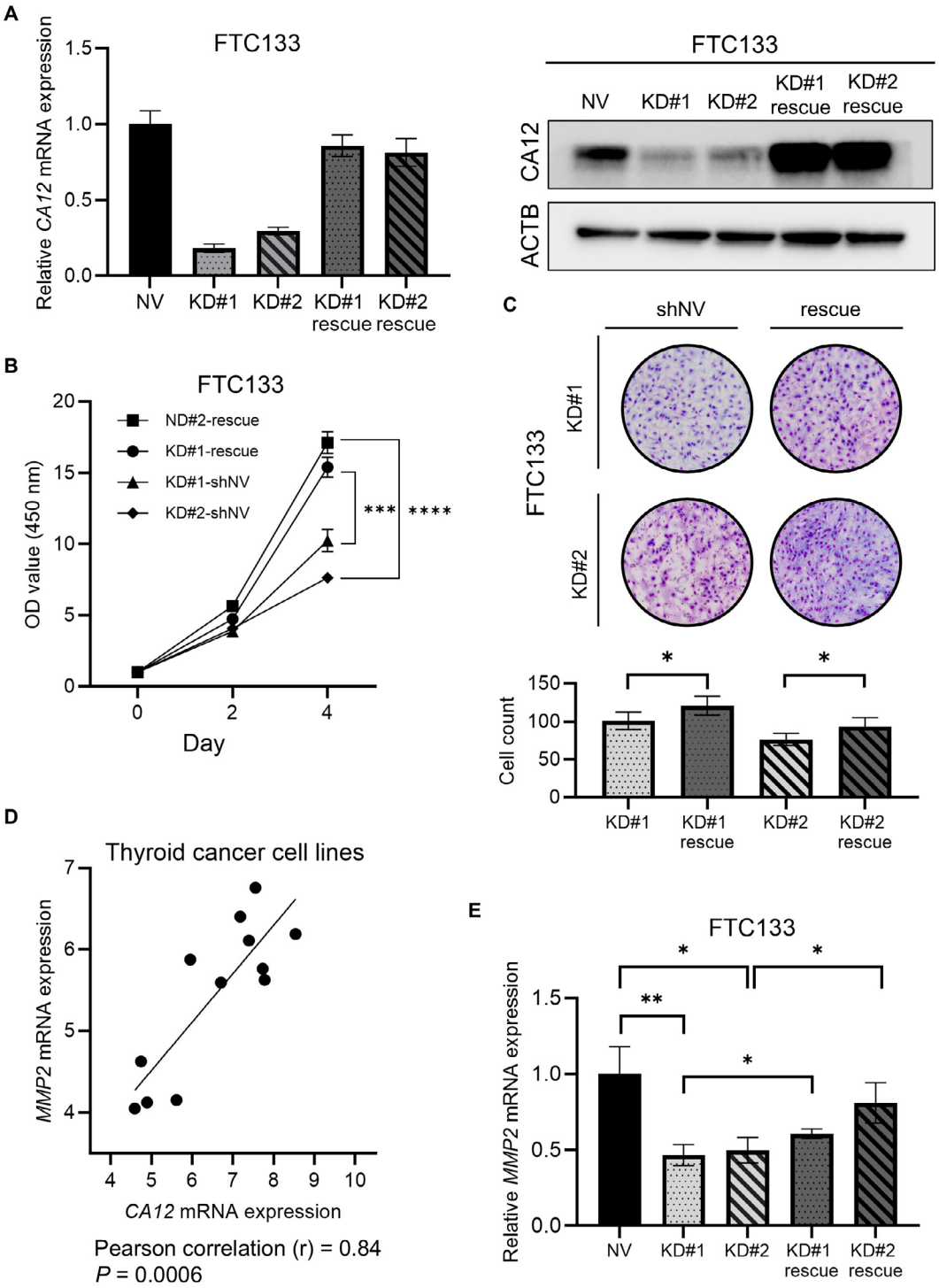

FIGURE 6 | CA12 rescue restores FTC cell invasion and proliferation, and regulates *MMP2* expression. (A) Validation of rescued CA12 expression in FTC133 cells, confirmed by RT-qPCR (left) and western blotting (right). (B) Cell proliferation assay. (C) Matrigel invasion assay. Representative images of infiltrating cells are shown. Infiltrating cells were counted in five random fields per well and plotted. (D) Correlation between CA12 and MMP2 mRNA in thyroid cancer cell lines. (E) Bar graph showing CA12 mRNA (top) and MMP2 mRNA (bottom) expression in knockdown and rescue cells in FTC133 (left) and FTC238 (right). Asterisks indicate significant differences (Student's *t*-test): $^{*}p < 0.05$, $^{**}p < 0.01$, $^{***}p < 0.001$, $^{****}p < 0.0001$. CA12, carbonic anhydrase 12; FTC, follicular thyroid carcinoma; MMP, matrix metalloproteinase.

therapeutic targets for metastatic FTC. The MI subtype of FTC has been studied using bulk RNA-seq or spatial transcriptomics [15, 19, 20], whereas highly aggressive subtypes, such as WI and metastatic lesions, remain less well investigated. In this study, we analyzed both primary and metastatic sites from highly aggressive FTC cases to identify therapeutic targets for metastasis. We identified *CA12* as a novel candidate prognostic marker and therapeutic target for FTC with metastasis.

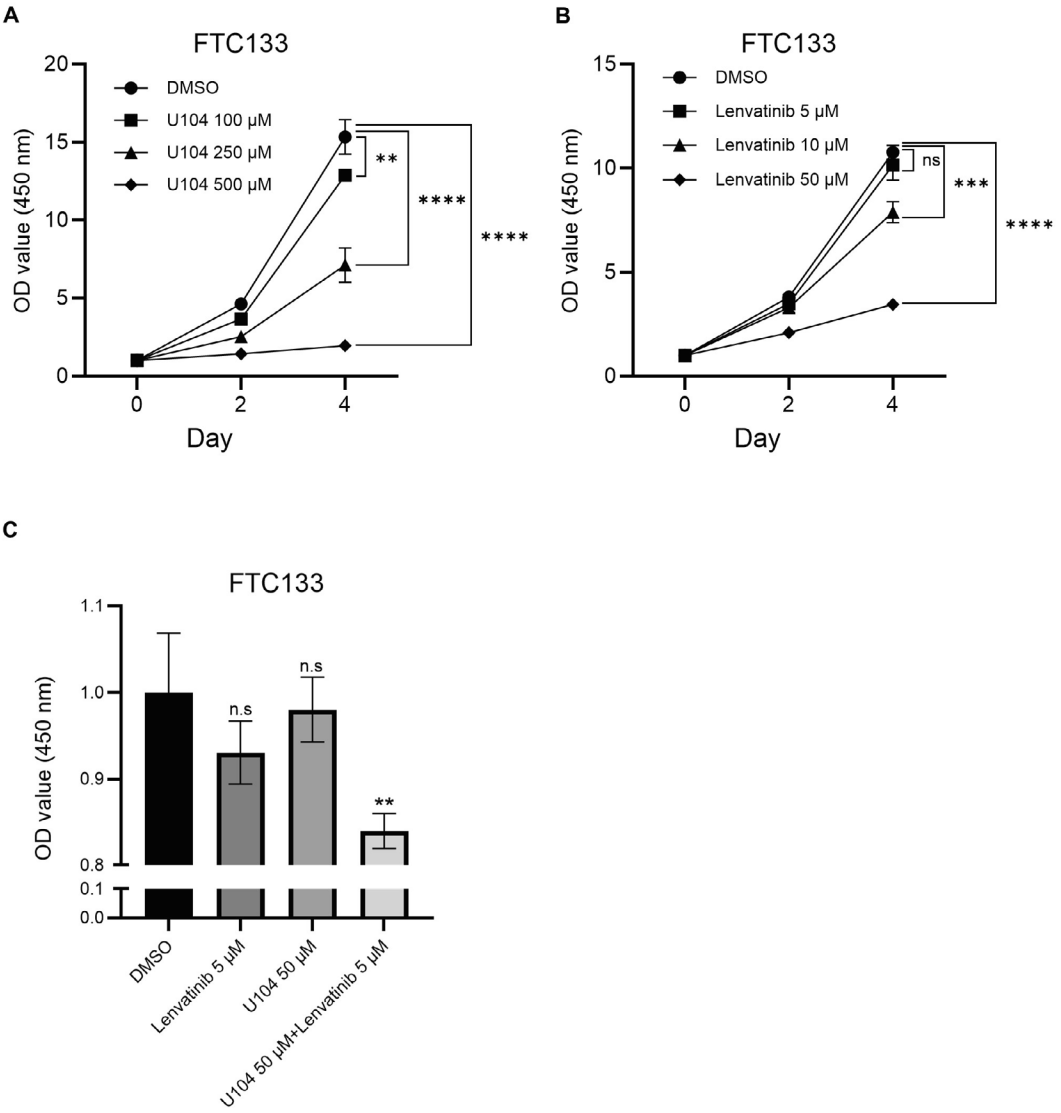

FIGURE 7 | CA12 inhibitor U104 and its combination with lenvatinib inhibit FTC cell proliferation. (A, B) Cell proliferation assays showing the dose-dependent effects of U104 (A) and lenvatinib (B) on FTC133 cells. (C) Synergistic effects of combining U104 and lenvatinib on FTC133 cell proliferation. Asterisks indicate significant differences (Student's *t*-test): $^{**}p < 0.01$, $^{***}p < 0.001$, $^{****}p < 0.0001$. CA12, carbonic anhydrase 12; FTC, follicular thyroid carcinoma.

CA belongs to a superfamily of metalloenzymes that catalyze the conversion of CO_2 to bicarbonate and protons. Humans possess 15 CA isoforms, categorized by their cellular localization. CA12 is located on the cell membrane and plays a role in pH regulation [13]. Although CA12 expression is reportedly elevated in several malignancies [21], our study is the first to perform an IHC analysis of CA12 in FTC. CA12 expression was significantly higher in FTC than in FA. MI FTC is associated with a favorable long-term prognosis and low recurrence and metastasis rate [22, 23]. We found that the MI subtype exhibited lower CA12 expression compared to other aggressive histopathological subtypes, such as the WI and EA subtypes. Furthermore, by stratifying the 50 FTC cases into CA12-high and CA12-low groups, we demonstrated that elevated CA12 expression was associated with poorer DFS. Notably, multivariate analysis identified high CA12 expression as an independent prognostic factor for DFS, exceeding the predictive value of histopathological type and tumor size. Current guidelines recommend stratifying therapy based on postoperative histopathological type [4]; however, CA12 expression may provide a more useful marker for treatment decisions.

The observation of high CA12 expression among FA cases is suggestive of a latent malignant potential leading to future progression to FTC. HE staining is insufficient to identify FA with malignant potential; however, CA12 immunostaining may serve as a crucial molecular tool to reveal this latent malignant risk. To verify clinical utility, further research would be necessary. For example, the long-term follow-up of numerous FA cases would reveal whether high CA12 expression predicts recurrence or metastasis, which is evidence of malignant potential.

We investigated the role of CA12 in vitro. CA12 was expressed in FTC cell lines (FTC133 and FTC238), but not in other thyroid cancer cell lines. Previous studies reported that CA12 contributes to the malignancy of various cancer types, including

breast cancer [24, 25], melanoma [26], and brain cancer [27]. Consistent with previous studies, our results showed that CA12 knockdown significantly suppressed the proliferation, invasion, and migration of FTC. Restoring CA12 expression rescued the proliferation and invasion of FTC133 cells. Notably, our data revealed a positive correlation between CA12 and MMP2 expression in thyroid carcinoma cell lines. MMP2, a member of the gelatinase subgroup of matrix metalloproteinases, plays a critical role in the degradation of the extracellular matrix (ECM) [28]. Its expression is higher in FTC than FA [29–31] and correlates with poor prognosis [31, 32]. It promotes tumor invasion and metastasis by degrading ECM components, enabling cancer cells to spread and promoting angiogenesis [33]. We found that CA12 knockdown decreased MMP2 expression, whereas CA12 rescue restored it. Given the function of MMP2 in promoting FTC cell invasion [34–36], CA12 may promote FTC invasion by positively regulating MMP2 expression.

We investigated the pharmacological effects of CA12 inhibition in vitro. Various CA inhibitors that target metabolism and the tumor microenvironment have been developed [13]. One of these, ureido-substituted benzenesulfonamides, showed antimetastatic activity in a model of breast cancer metastasis and is thought to be a candidate for the development of a novel antimetastatic drug [37]. Therefore, we investigated the effects of the CA12 inhibitor U104, a ureido-substituted benzenesulfonamide. U104 inhibits tumor growth in various cancer types [38–40]. U104 has already passed a phase I clinical trial in patients with advanced solid tumors [41]. Consistent with previous reports, we observed that U104 inhibited FTC133 cell proliferation in a dose-dependent manner. Furthermore, our findings demonstrate that U104 enhances the therapeutic efficacy of lenvatinib, a molecularly targeted agent used to treat metastatic FTC. A combination trial of U104 and gemcitabine has been initiated in patients with metastatic pancreatic ductal carcinoma (NCT03450018). In our study, U104 inhibited FTC133 proliferation in a dose-dependent manner and enhanced the therapeutic efficacy of low-dose lenvatinib. Although lenvatinib is used to treat metastatic FTC, adverse events, such as hypertension and proteinuria, restrict the use of the standard dose [17]. Thus, combination therapy with U104 and lenvatinib may represent a novel treatment for metastatic FTC.

Although this study identified CA12 expression as a potential biomarker using RNA-seq analysis on FTC, its limitations warrant further consideration. Due to the limited sample size of 50 cases, no significant difference in OS rate was observed. Future studies require validation with a larger number of cases.

Author Contributions

Masashi Tanida: conceptualization, data curation, formal analysis, investigation, software, writing – original draft. **Tsuyoshi Takashima:** conceptualization, investigation, writing – review and editing. **Shinichiro Tahara:** investigation. **Masaharu Kohara:** investigation. **Haruka Kanai:** data curation. **Masami Suzuki:** investigation. **Motoyuki Suzuki:** data curation. **Mitsuyoshi Hirokawa:** data curation. **Ayana Suzuki:** data curation. **Shinya Sato:** data curation. **Daisuke Okuzaki:** formal analysis, software. **Satoshi Nojima:** investigation. **Takahiro Matsui:** investigation. **Hidenori Inohara:** conceptualization, supervision. **Eiichi Morii:** conceptualization, formal analysis, software, supervision, writing – review and editing.

Acknowledgments

We thank Ms. Etsuko Fujinami, Ms. Takako Sawamura and Ms. Megumi Nihei (Department of Pathology, Graduate School of Medicine, The University of Osaka) and Ms. Miyuki Towata (Yamashita Thyroid Hospital) for their technical assistance. We used the bioresearch sources of MISSION shRNA library in the Center for Medical Research and Education, Graduate School of Medicine, The University of Osaka.

Disclosure

Eiichi Morii is the Editorial Board Member of Cancer Science. Other authors of this manuscript are not the current Editor or Editorial Board Members of Cancer Science.

Ethics Statement

Approval of the research protocol by an Institutional Review Board: This research was approved by the Ethics Review Board of the Graduate School of Medicine, The University of Osaka (No. 849).

Consent

The authors have nothing to report.

Conflicts of Interest

The authors declare no conflicts of interest.

References

1. L. Boucai, M. Zafereo, and M. E. Cabanillas, "Thyroid Cancer: A Review," *JAMA* 331, no. 5 (2024): 425–435, https://doi.org/10.1001/jama.2023.26348.

2. M. T. Stegenga, L. Oudijk, E. F. S. van Velsen, et al., "Impact of Reclassification of Oncocytic and Follicular Thyroid Carcinoma by the 2022 WHO Classification," *Journal of Clinical Endocrinology and Metabolism* 110, no. 5 (2025): e1343–e1350, https://doi.org/10.1210/clinem/dgae581.

3. C. C. Juhlin and Z. W. Baloch, "Pitfalls in Thyroid Fine-Needle Aspiration Cytopathology: An Approach to Atypical Findings," *Acta Cytologica* 68, no. 3 (2024): 179–193, https://doi.org/10.1159/000535907.

4. G. Grani, L. Lamartina, C. Durante, S. Filetti, and D. S. Cooper, "Follicular Thyroid Cancer and Hurthle Cell Carcinoma: Challenges in Diagnosis, Treatment, and Clinical Management," *Lancet Diabetes & Endocrinology* 6, no. 6 (2018): 500–514, https://doi.org/10.1016/S2213-8587(17)30325-X.

5. S. Shah and L. Boucai, "Effect of Age on Response to Therapy and Mortality in Patients With Thyroid Cancer at High Risk of Recurrence," *Journal of Clinical Endocrinology and Metabolism* 103, no. 2 (2018): 689–697, https://doi.org/10.1210/jc.2017-02255.

6. M. H. Wu, Y. Y. Lee, Y. L. Lu, and S. F. Lin, "Risk Factors and Prognosis for Metastatic Follicular Thyroid Cancer," *Front Endocrinol (Lausanne)* 13 (2022): 791826, https://doi.org/10.3389/fendo.2022.791826.

7. A. K. Siraj, S. K. Parvathareddy, P. Annaiyappanaidu, et al., "Male Sex Is an Independent Predictor of Recurrence-Free Survival in Middle Eastern Papillary Thyroid Carcinoma," *Front Endocrinol (Lausanne)* 13 (2022): 777345, https://doi.org/10.3389/fendo.2022.777345.

8. J. Ding, W. Wu, J. Fang, J. Zhao, and L. Jiang, "Male Sex Is Associated With Aggressive Behaviour and Poor Prognosis in Chinese Papillary Thyroid Carcinoma," *Scientific Reports* 10, no. 1 (2020): 4141, https://doi.org/10.1038/s41598-020-60,199-9.

9. J. Shen, M. Yan, L. Chen, et al., "Prognosis and Influencing Factors of Follicular Thyroid Cancer," *Cancer Medicine* 13, no. 1 (2024): e6727, https://doi.org/10.1002/cam4.6727.

10. H. Yamazaki, K. Sugino, R. Katoh, et al., "Role of the Degree of Vascular Invasion in Predicting Prognosis of Follicular Thyroid Carcinoma," *Journal of Clinical Endocrinology and Metabolism* 109, no. 5 (2024): 1291–1300, https://doi.org/10.1210/clinem/dgad689.

11. L. S. Hellgren, A. Stenman, J. O. Paulsson, et al., "Prognostic Utility of the Ki-67 Labeling Index in Follicular Thyroid Tumors: A 20-Year Experience From a Tertiary Thyroid Center," *Endocrine Pathology* 33, no. 2 (2022): 231–242, https://doi.org/10.1007/s12022-022-09714-4.

12. E. Macerola, A. M. Poma, P. Vignali, et al., "Predictive Biomarkers in Thyroid Cancer," *Frontiers in Oncology* 12 (2022): 901004, https://doi.org/10.3389/fonc.2022.901004.

13. A. angeli, F. Carta, A. Nocentini, et al., "Carbonic Anhydrase Inhibitors Targeting Metabolism and Tumor Microenvironment," *Metabolites* 10, no. 10 (2020): 412, https://doi.org/10.3390/metabo10100412.

14. J. Haase, D. Misiak, M. Bauer, et al., "IGF2BP1 Is the First Positive Marker for Anaplastic Thyroid Carcinoma Diagnosis," *Modern Pathology* 34, no. 1 (2021): 32–41, https://doi.org/10.1038/s41379-020-0630-0.

15. S. K. Yoo, S. Lee, S. J. Kim, et al., "Comprehensive Analysis of the Transcriptional and Mutational Landscape of Follicular and Papillary Thyroid Cancers," *PLoS Genetics* 12, no. 8 (2016): e1006239, https://doi.org/10.1371/journal.pgen.1006239.

16. S. X. Ge, E. W. Son, and R. Yao, "iDEP: An Integrated Web Application for Differential Expression and Pathway Analysis of RNA-Seq Data," *BMC Bioinformatics* 19, no. 1 (2018): 534, https://doi.org/10.1186/s12859-018-2486-6.

17. M. Schlumberger, M. Tahara, L. J. Wirth, et al., "Lenvatinib Versus Placebo in Radioiodine-Refractory Thyroid Cancer," *New England Journal of Medicine* 372, no. 7 (2015): 621–630, https://doi.org/10.1056/NEJMoa1406470.

18. T. E. Luvhengo, I. Bombil, A. Mokhtari, et al., "Multi-Omics and Management of Follicular Carcinoma of the Thyroid," *Biomedicine* 11, no. 4 (2023): 1217, https://doi.org/10.3390/biomedicines11041217.

19. A. Suzuki, S. Nojima, S. Tahara, et al., "Identification of Invasive Subpopulations Using Spatial Transcriptome Analysis in Thyroid Follicular Tumors," *Journal of Pathology and Translational Medicine* 58, no. 1 (2024): 22–28, https://doi.org/10.4132/jptm.2023.11.21.

20. V. Condello, J. O. Paulsson, J. Zedenius, A. Nasman, and C. C. Juhlin, "Spatial Transcriptomics in a Case of Follicular Thyroid Carcinoma Reveals Clone-Specific Dysregulation of Genes Regulating Extracellular Matrix in the Invading Front," *Endocrine Pathology* 35, no. 2 (2024): 122–133, https://doi.org/10.1007/s12022-024-09798-0.

21. A. Waheed and W. S. Sly, "Carbonic Anhydrase XII Functions in Health and Disease," *Gene* 623 (2017): 33–40, https://doi.org/10.1016/j.gene.2017.04.027.

22. P. Goffredo, K. Cheung, S. A. Roman, and J. A. Sosa, "Can Minimally Invasive Follicular Thyroid Cancer Be Approached as a Benign Lesion?: A Population-Level Analysis of Survival Among 1200 Patients," *Annals of Surgical Oncology* 20, no. 3 (2013): 767–772, https://doi.org/10.1245/s10434-012-2697-4.

23. K. Sugino, K. Ito, M. Nagahama, et al., "Prognosis and Prognostic Factors for Distant Metastases and Tumor Mortality in Follicular Thyroid Carcinoma," *Thyroid* 21, no. 7 (2011): 751–757, https://doi.org/10.1089/thy.2010.0353.

24. G. Guerrini, M. Criscuoli, I. Filippi, A. Naldini, and F. Carraro, "Inhibition of Smoothened in Breast Cancer Cells Reduces CAXII Expression and Cell Migration," *Journal of Cellular Physiology* 233, no. 12 (2018): 9799–9811, https://doi.org/10.1002/jcp.26947.

25. M. J. Hsieh, K. S. Chen, H. L. Chiou, and Y. S. Hsieh, "Carbonic Anhydrase XII Promotes Invasion and Migration Ability of MDA-MB-231 Breast Cancer Cells Through the p38 MAPK Signaling Pathway," *European Journal of Cell Biology* 89, no. 8 (2010): 598–606, https://doi.org/10.1016/j.ejcb.2010.03.004.

26. G. Giuntini, F. Coppola, A. Falsini, et al., "Role of the Hedgehog Pathway and CAXII in Controlling Melanoma Cell Migration and Invasion in Hypoxia," *Cancers (Basel)* 14, no. 19 (2022): 4776, https://doi.org/10.3390/cancers14194776.

27. G. Li, T. W. Chen, A. C. Nickel, et al., "Carbonic Anhydrase XII Is a Clinically Significant, Molecular Tumor-Subtype Specific Therapeutic Target in Glioma With the Potential to Combat Invasion of Brain Tumor Cells," *Oncotargets and Therapy* 14 (2021): 1707–1718, https://doi.org/10.2147/OTT.S300623.

28. M. Wolosowicz, S. Prokopiuk, and T. W. Kaminski, "The Complex Role of Matrix Metalloproteinase-2 (MMP-2) in Health and Disease," *International Journal of Molecular Sciences* 25, no. 24 (2024): 13691, https://doi.org/10.3390/ijms252413691.

29. K. Cho Mar, T. Eimoto, H. Tateyama, Y. Arai, Y. Fujiyoshi, and M. Hamaguchi, "Expression of Matrix Metalloproteinases in Benign and Malignant Follicular Thyroid Lesions," *Histopathology* 48, no. 3 (2006): 286–294, https://doi.org/10.1111/j.1365-2559.2005.02325.x.

30. H. Tan, K. Ye, Z. Wang, and H. Tang, "Clinicopathologic Evaluation of Immunohistochemical CD147 and MMP-2 Expression in Differentiated Thyroid Carcinoma," *Japanese Journal of Clinical Oncology* 38, no. 8 (2008): 528–533, https://doi.org/10.1093/jjco/hyn065.

31. S. Sanii, H. Saffar, H. M. Tabriz, M. Qorbani, V. Haghpanah, and S. M. Tavangar, "Expression of Matrix Metalloproteinase-2, but Not Caspase-3, Facilitates Distinction Between Benign and Malignant Thyroid Follicular Neoplasms," *Asian Pacific Journal of Cancer Prevention* 13, no. 5 (2012): 2175–2178, https://doi.org/10.7314/apjcp.2012.13.5.2175.

32. H. Liang, Y. Zhong, Z. Luo, et al., "Diagnostic Value of 16 Cellular Tumor Markers for Metastatic Thyroid Cancer: An Immunohistochemical Study," *Anticancer Research* 31, no. 10 (2011): 3433–3440.

33. C. M. Overall and C. Lopez-Otin, "Strategies for MMP Inhibition in Cancer: Innovations for the Post-Trial Era," *Nature Reviews. Cancer* 2, no. 9 (2002): 657–672, https://doi.org/10.1038/nrc884.

34. V. Kalhori and K. Tornquist, "MMP2 and MMP9 Participate in S1P-Induced Invasion of Follicular ML-1 Thyroid Cancer Cells," *Molecular and Cellular Endocrinology* 404 (2015): 113–122, https://doi.org/10.1016/j.mce.2015.01.037.

35. P. Saejia, K. Lirdprapamongkol, J. Svasti, and N. M. Parichartanakul, "Perfluorooctanoic Acid Enhances Invasion of Follicular Thyroid Carcinoma Cells Through NF-kappaB and Matrix Metalloproteinase-2 Activation," *Anticancer Research* 39, no. 5 (2019): 2429–2435, https://doi.org/10.21873/anticanres.13360.

36. M. W. Yeh, J. P. Rougier, J. W. Park, et al., "Differentiated Thyroid Cancer Cell Invasion Is Regulated Through Epidermal Growth Factor Receptor-Dependent Activation of Matrix Metalloproteinase (MMP)-2/Gelatinase A," *Endocrine-Related Cancer* 13, no. 4 (2006): 1173–1183, https://doi.org/10.1677/erc.1.01226.

37. F. Pacchiano, F. Carta, P. C. McDonald, et al., "Ureido-Substituted Benzenesulfonamides Potently Inhibit Carbonic Anhydrase IX and Show Antimetastatic Activity in a Model of Breast Cancer Metastasis," *Journal of Medicinal Chemistry* 54, no. 6 (2011): 1896–1902, https://doi.org/10.1021/jm101541x.

38. K. Zhao, X. Wang, Y. Jin, et al., "LncRNA ZNF674-AS1 Drives Cell Growth and Inhibits Cisplatin-Induced Pyroptosis via Up-Regulating CA9 in Neuroblastoma," *Cell Death & Disease* 15, no. 1 (2024): 5, https://doi.org/10.1038/s41419-023-06394-8.

39. A. Riemann, A. Guttler, V. Haupt, et al., "Inhibition of Carbonic Anhydrase IX by Ureidosulfonamide Inhibitor U104 Reduces Prostate

Cancer Cell Growth, but Does Not Modulate Daunorubicin or Cisplatin Cytotoxicity," *Oncology Research* 26, no. 2 (2018): 191–200, https://doi.org/10.3727/096504017X14965111926391.

40. A. Guttler, K. Theuerkorn, A. Riemann, et al., "Cellular and Radiobiological Effects of Carbonic Anhydrase IX in Human Breast Cancer Cells," *Oncology Reports* 41, no. 4 (2019): 2585–2594, https://doi.org/10.3892/or.2019.7001.

41. P. C. McDonald, S. chia, P. L. Bedard, et al., "A Phase 1 Study of SLC-0111, a Novel Inhibitor of Carbonic Anhydrase IX, in Patients With Advanced Solid Tumors," *American Journal of Clinical Oncology* 43, no. 7 (2020): 484–490, https://doi.org/10.1097/COC.0000000000000691.

Supporting Information

Additional supporting information can be found online in the Supporting Information section. **Table S1:** The list of eight cases performed RNA-seq. **Table S2:** Clinicopathological features of follicular thyroid tumors ($n = 75$). **Table S3:** DEGs between primary site vs. normal thyroid tissue. **Table S4:** DEGs between metastasis site vs. normal thyroid tissue. **Table S5:** Correlation between CA12 and MMP2 expression in various thyroid carcinoma cell lines.